

Brain pericytes derived from human pluripotent stem cells retain vascular and phagocytic functions under hypoxia

Mingzi Zhang, Youbin Kim, Allison Bosworth, Julia Tcw, Lina R Nih, Kassandra Kisler, Abhay P Sagare, Ruslan Rust



The banner features a white laboratory incubator on the left. To its right, the text "You Don't Need Reproducible Research" is written in white on a dark blue background. Below this, the slogan "UNTIL YOU DO." is displayed in large, bold, white capital letters. At the bottom, a green bar contains the text "Minimize uncertainty with PHCbi brand products" in white. On the far right, the PHCbi logo is shown, consisting of the lowercase letters "phcbi" in a blue sans-serif font.

Brain pericytes derived from human pluripotent stem cells retain vascular and phagocytic functions under hypoxia

Mingzi Zhang^{1,2,†}, Youbin Kim^{1,2,†}, Allison Bosworth^{1,2}, Julia Tcw³, Lina R. Nih⁴, Kassandra Kisler^{1,2}, Abhay P. Sagare^{1,2}, Ruslan Rust^{*1,2,‡}

¹Department of Physiology and Neuroscience, University of Southern California, Los Angeles, CA 90033, United States

²Zilkha Neurogenetic Institute, Keck School of Medicine, University of Southern California, Los Angeles, CA 90033, United States

³Department of Pharmacology, Physiology & Biophysics, Chobanian & Avedisian School of Medicine, Boston University, Boston, MA 02118, United States

⁴Department of Brain Health, Kirk Kerkorian School of Medicine, University of Nevada, Las Vegas, NV 89154, United States

*Corresponding author: Department of Physiology and Neuroscience, Keck School of Medicine, University of Southern California, 1501 San Pablo Street, Room 341, Los Angeles, CA 90033, USA (rtrust@usc.edu).

†M. Zhang and Y. Kim contributed equally to this work.

Abstract

Background: The integrity and function of the blood-brain barrier (BBB) are largely regulated by pericytes. Pericyte deficiency leads to BBB breakdown and neurological dysfunction in major neurological disorders including stroke and Alzheimer's disease (AD). Transplantation of pericytes derived from induced pluripotent stem cells (iPSC-PC) has been shown to restore the BBB and improve functional recovery in mouse models of stroke and pericyte deficiency. However, the molecular profile and functional properties of iPSC-PC under hypoxic conditions, similar to those found in ischemic and neurodegenerative diseases remain largely unexplored.

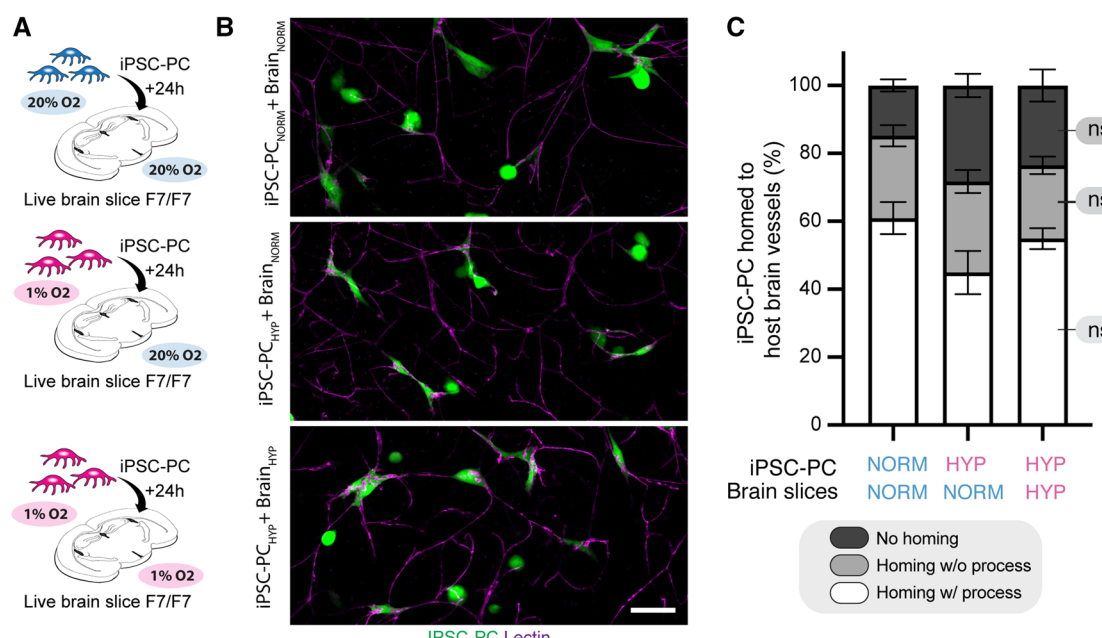
Methods: We examined iPSC-PC under hypoxia to assess molecular marker expression, proliferation, ability to home to brain vessels, and uptake of amyloid beta (A β).

Results: iPSC-PC under severe hypoxia retain essential functional properties, including key molecular markers, proliferation rates, and the ability to migrate to host brain vessels via function-associated PDGFRB-PDGF-BB signaling. Additionally, we show that iPSC-PC exhibit similar clearance of A β neurotoxins from AD mouse brain sections under both normoxic and hypoxic conditions.

Conclusions: These findings suggest that iPSC-PC functions are largely resilient to hypoxia, highlighting their potential as a promising cell source for treating ischemic and neurodegenerative disorders.

Key words: cell therapy; mural cells; neurodegeneration; ischemia; stroke.

Graphical abstract



Received: 30 April 2025; Accepted: 29 July 2025.

© The Author(s) 2025. Published by Oxford University Press.

This is an Open Access article distributed under the terms of the Creative Commons Attribution License (<https://creativecommons.org/licenses/by/4.0/>), which permits unrestricted reuse, distribution, and reproduction in any medium, provided the original work is properly cited.

Significance statement

Pericytes are critical support cells that help to maintain the brain's protective barrier and clear toxic proteins linked to neurological diseases. When these cells are lost, the brain becomes more vulnerable to damage, as seen in stroke and Alzheimer's disease. Stem cell-derived pericytes offer a promising therapeutic approach, but it is unclear whether they retain their key functional properties in low-oxygen conditions common in diseased brain tissue. Our study shows that induced pluripotent stem cell-derived pericytes retain key molecular and functional properties under severe hypoxia, supporting their potential as a treatment option for ischemic and neurodegenerative disorders.

Introduction

Pericytes are mural cells that wrap around the endothelium, playing an important role in maintaining blood–brain barrier (BBB) integrity, regulating blood flow, promoting vessel maturation, and clearing toxic proteins in the brain.^{1–8} Loss of pericytes leads to BBB breakdown, which is associated with neuronal dysfunction and poor outcomes in major neurological disorders, including stroke and Alzheimer's disease (AD) in both mice and humans.^{9–12}

Recently, protocols have been developed to generate pericytes from induced pluripotent stem cells (iPSC-PCs).^{13–15} Transplantation of iPSC-PCs has shown to enhance BBB integrity in mouse models of ischemic stroke^{16,17} and pericyte-deficient mice.¹⁵ Furthermore, iPSC-PCs exhibit a transcriptomic and proteomic signature similar to primary human brain pericytes.^{13–15}

Despite these advances, molecular profiling of iPSC-PCs has largely been explored under normoxic conditions, even though cell therapy applications often involve reduced cerebral blood flow causing hypoxic environments, such as those seen after ischemic stroke¹⁸ or in AD.¹⁹ It remains unclear how hypoxia influences the molecular profile and functional properties of iPSC-PCs.

In this study, we demonstrate that iPSC-PCs retain the expression of canonical markers and show similar proliferation rates under severe hypoxia *in vitro*. Transcriptomic profiling revealed that while hypoxia-related pathways were upregulated, key functional components of iPSC-PCs, including tight junction and adhesion junction molecules, remained unaffected by hypoxia. Functionally, hypoxic iPSC-PC retained the ability to migrate toward host brain capillaries, extend processes, and form hybrid human–mouse microvessels with functional associations. Additionally, normoxic and hypoxic iPSC-PCs exhibited comparable abilities to phagocytose amyloid beta (A β) neurotoxins from AD mouse brain sections.

Methods

Mice

Platelet-derived growth factor receptor β mutant mice, Pdgfrb $^{F/F}$ on 129S1/SvlM background were used for ex vivo and in vivo studies, as described below. Mice express PDGFR β with 7 point mutations that disrupt signal transduction pathways, including residue 578 (Src), residue 715 (Grb2), residues 739 and 750 (PI3K), residue 770 (RasGAP), residue 1008 (SHP-2), by changing the tyrosine to phenylalanine, and residue 1020 (PLC γ), where tyrosine was mutated to isoleucine, as reported.²⁰ Pdgfrb $^{F/F}$ mice express mutant PDGFR β exclusively in perivascular mural cells including pericytes, and not in neurons, astrocytes, or brain endothelial cells.^{3,21} All procedures received approval (Protocol 20621) from the Institutional Animal Care and Use Committee at the University of Southern California in accordance with US National

Institutes of Health guidelines and were conducted following the ARRIVE guidelines.²²

Cell culture

Human iPSC cultures were generated from skin fibroblasts as previously described.²³ Human iPSC-PC were generated via neural crest cell (NCC) intermediates following previously established protocols.^{13,14} Briefly, iPSC were cultured on growth factor-reduced matrigel (Corning, 356230) in mTeSR Plus medium (StemCell Technologies, 100-0276). NCC differentiation was induced using STEMdiff Neural Crest Differentiation Kit (StemCell Technologies, 08610). Prior to differentiation, iPSCs were washed with Phosphate-Buffered Saline (PBS), dissociated with Accutase (Thermo Fisher, A1110501) for 5 min, centrifuged at 200g for 4 min, and counted using a Countess 3 (Thermo Fisher, AMQAX2000). Induced pluripotent stem cells were then seeded at a density of $0.75\text{--}1 \times 10^5$ cells/cm 2 in mTeSR plus (StemCell Technologies, 1000276) supplemented with 10 mM Y-27632 (Tocris, 1254). Seeding densities were adjusted for each iPSC line to ensure 100% confluence at differentiation days 3–4. Media were changed daily using NCC media from the STEMdiff kit. After 6 days of differentiation, iPSC-NCC were dissociated using Accutase for 5 min and purified using EasySep Release Human PSC-derived NCC Positive Selection Kit (StemCell Technologies, 100-0047), following the manufacturer's instructions.

Neural crest cells were further differentiated to iPSC-PC. Induced pluripotent stem cell-derived NCCs were replated onto matrigel-coated 6-well plates at a 1:2 split ratio, and pericyte medium (ScienCell, 1201) was introduced the following day. Media were changed daily, and once cells reached 70%–80% confluence, they were passaged using 0.05% Trypsin/EDTA (Thermo Fisher, 25300054) and replated onto poly-L-lysine (PLL)-coated dishes. After 14 days of differentiation, iPSC-PCs were transferred onto glass coverslips for subsequent imaging.

For hypoxia induction, iPSC-PCs from the same cell line were cultured under either normoxic (21% O $_2$) or hypoxic (1% O $_2$) conditions for up to 7 days using a Hypoxia Incubator Chamber (STEMCELL Technologies, 27310) according to the manufacturer's instructions. After hypoxia treatment, cells were either fixed for immunocytochemical analysis, processed for RNA sequencing, or added to brain tissue for ex vivo assays.

Immunostaining

Pericytes from induced pluripotent stem cells were plated on glass coverslips and maintained in culture before fixation with 4% Paraformaldehyde (PFA) for 10 min. Cells were then rinsed twice with sterile PBS, followed by 3 consecutive 5-min washes in PBS. Blocking was performed for at least 1 h in PBS containing 5% donkey serum and 0.5% Triton X-100. Cells were incubated overnight at 4°C with primary antibodies against

PDGFR β (R&D Systems, AF385, 1:100, Goat) and NG2 (Sigma, AB5320, 1:500, Rabbit) diluted in PBS supplemented with 5% donkey serum (PBS-D). The following day, cells underwent five 8-min washes in PBS before incubation with secondary antibodies (Invitrogen, A32794, Alexa Fluor Plus 555, 1:300, and Invitrogen, A32860, Alexa Fluor Plus 680, 1:300, Donkey) in PBS-D for 1-2 h at room temperature. After 4 additional 8-min PBS washes, coverslips were mounted with DAPI-containing mounting medium (Southern Biotech, 0100-20) and imaged using a Nikon A1R confocal microscopy system with NIS-Elements software, using 10 \times , 20 \times , and 60 \times objectives.

Quantification of PDGFRB- and NG2-positive cells

All samples were stained and imaged using identical image acquisition settings; images were processed and analyzed using ImageJ (Fiji), similar to previous studies.²⁴ Fluorescence signal from the marker of interest (PDGFRB, NG2) was thresholded using Otsu thresholding plugin²⁵ in each image. The thresholding was performed in the same manner for all samples. Analyze Particles function was used to determine the number of marker-positive cells. To calculate the percentage of positive cells, the number of marker-positive cells was normalized to the total DAPI-positive nuclei count for each image. DAPI-stained nuclei were used to identify individual cells and to normalize pericyte marker expression. Overlap between NG2 or PDGFRB signals and surrounding DAPI+ nuclei was assessed to determine marker-positive cells. Investigators were blinded to sample identity during analysis to avoid bias. Regions with lower cell density were preferentially analyzed to facilitate individual cell identification and minimize segmentation errors in high-density areas.

RNA sequencing and analysis

Total RNA from iPSC-PC was extracted using RNeasy RNA isolation kit (Qiagen, 73404), including DNase treatment to remove residual genomic DNA, according to the manufacturer's instruction, and as previously described.²⁶⁻³⁰ All samples had an RIN value greater than 8.5. Library preparation, sequencing, read processing, alignment, and read counting were performed at the USC Norris Cancer Center Molecular Genomics Core. For library preparation, the TruSeq Stranded RNA kit (Illumina Inc.) was used following the manufacturer's protocol. mRNA was purified via polyA selection, chemically fragmented, and transcribed into cDNA before adapter ligation. Initial data preprocessing, including quality control, adapter trimming, and filtering of low-quality reads, was performed using Galaxy open source platform. Reads were aligned to the human genome (GRCh38) using STAR aligner with default parameters. RNA sequencing data analysis and gene set enrichment analysis were conducted as previously described^{27,28,31} and using standard guidelines with EdgeR³² and clusterProfiler 4.0³³ with default parameters, applying the Benjamini-Hochberg (BH) method for multiple testing correction.

Preparation and analysis of ex vivo living brain slices

We used acute living brain slice culture as a method to study iPSC-PC-vascular interactions in a physiologically relevant brain environment ex vivo. For this assay, iPSC-PCs were labeled with CellTracker Green CMFDA (Invitrogen, C7025) following the manufacturer's instructions, and cultured in either normoxic or hypoxic condition for 1 week before the

brain slice preparation. The 8-month-old *Pdgfrb*F7/F7 mice were retroorbitally injected with 80 μ L DyLight-649 labeled Lycopersicon esculentum lectin (Vector Laboratories, DL-1178-1)³ to identify blood vessels at least 15 min prior to euthanasia. Mice were deeply anaesthetized with 5% Isoflurane, then, rapidly decapitated and brain extracted into ice-cold Hibernate A minus Phenol Red medium (Transnetyx Tissue, HAPR500). Slice preparation was performed on a Leica VT1000S vibratome. Coronal slices (250 μ m) containing the hippocampus were then cut in ice-cold Hibernate A minus Phenol Red medium.

After sectioning, slices were maintained in homing medium containing DMEM (Gibco, 10569010), 5% FBS (Gibco, 16140-071), Pen-Strep (Gibco, 15140122), 2% platelet lysate (Stem Cell Technology, 200-0323), antioxidant (Sigma-Aldrich, A1345), GlutaMAX (Gibco, 35050061), Na-Pyruvate (Gibco, 11360070), CultureBoost (Cell Systems, 4CB-500), Pericyte Supplement (ScienCell, 1252). Subsequently, 50 000 iPSC-PCs were added on top of each brain slice and allowed to integrate with the tissue in an incubator maintained at 37°C in either normoxic or hypoxic conditions for 24 h. Brain slices were fixed in 4% PFA for 30 min, mounted on slides, coverslipped with mounting media and imaged on a Nikon A1R confocal microscopy system with NIS-Elements software control. The iPSC-PC on brain slices were scored as (1) being associated with a vessel and forming processes, (2) associated with a vessel without processes, or (3) not associated with a vessel.

Proximity ligation assay

The interactions of PDGF-BB and PDGFR β in the brain slices were determined by proximity ligation assay (PLA) using NaveniFlex Tissue GR Red (Navinci, 39220). After fixation and blocking, brain slices were incubated with rabbit anti-PDGF-BB IgG (Invitrogen, MA5-51346, 1:100) and goat anti-human PDGFR β IgG (R&D Systems, BAF385, 1:50) overnight at 4°C. Proximity ligation was then conducted following the manufacturer's instructions. Proximity ligation results in a fluorescence signal only when the PLA agent detects the antibodies for PDGFR β and PDGF-BB within close proximity, indicating likely colocalization of PDGFR β and PDGF-BB.

A β uptake assay from brain sections

Pericytes from induced pluripotent stem cells were labeled with CellTracker Green CMFDA (Invitrogen, C7025) and cultured in either normoxic or hypoxic conditions for 1 week before the brain slice preparation. Mice were transcardially perfused with cold PBS prior to tissue collection. Brains were fresh-frozen and stored at -80 °C. Cryosections (20 μ m) from 9- to 11-month-old 5xFAD mouse brains were mounted on PLL-coated coverslips and stored at -80 °C. For each experimental replicate, consecutive adjacent sections from the same brain region (cortex and hippocampus) were used across the 3 experimental groups. Prior to use, sections were thawed, rinsed with PBS, and incubated in pericyte culture medium (ScienCell) for 2 h at 37°C. Pericytes from induced pluripotent stem cells were seeded onto tissue sections at 100k cells/well, with "no-cell" controls included. Cultures were maintained for 24 h at 37°C. Sections were then fixed in 4% paraformaldehyde, permeabilized in PBS containing donkey serum and 0.075% Triton X-100, and stained with a pan-A β antibody (1:1200, Cell

Signaling Technology) followed by secondary antibody incubation. Coverslips were mounted using DAPI-containing mounting medium and imaged using a confocal microscope at 4 \times magnification. For analysis, images were binarized using a customized threshold and percentage of A β signal were quantified in cortex and hippocampus using ImageJ (Fiji).

Statistics

Data are presented as mean \pm SEM. All analyses were performed using GraphPad Prism 10 or R Studio 3.6.0. Normality of the data was tested using the Shapiro-Wilk test. For comparisons between 2 groups, an unpaired 2-tailed Student's *t*-test was used for independent samples, and a paired *t*-test was applied for repeated measures. For multiple group comparisons, a 1-way analysis of variance (ANOVA) was used, followed by Tukey's post hoc test for pairwise comparisons. For repeated measures across different groups, a repeated measures mixed model was applied. For quantification of gene expression changes in transcriptomic data, differential gene expression analysis was performed using EdgeR, and multiple testing correction was applied using the BH method. Statistical significance was defined as * P <.05, ** P <.01, and *** P <.001.

Results

Hypoxia does not impact the growth or canonical marker expression in iPSC-PC

We generated pericyte-like cells from iPSCs via NCC intermediates as previously described,¹⁵ and exposed iPSC-PC to hypoxia for 1 week (iPSC-PC_{HYP}). We used a control group of iPSC-PC under normoxic conditions (iPSC-PC_{NORM}). We confirmed that O₂ levels were stably reduced to 1% oxygen in the hypoxic group throughout the experiment (Figure 1B). Proliferation rates of iPSC-PC_{HYP} were similar to those of control iPSC-PC_{NORM} at 3, 5, and 7 days after hypoxia induction (Figure 1C). We observed no significant differences in the percentage of total cells expressing the canonical pericyte markers NG2 (iPSC-PC_{HYP}: 83.7%; iPSC-PC_{NORM}: 79.4%, P >.05) and PDGFRB (iPSC-PC_{HYP}: 82.1%; iPSC-PC_{NORM}: 85.7%, P >.05) in fluorescence immunostaining (Figure 1E and F). Additionally, the fluorescence signal intensity of NG2 and PDGFRB expressing cells was comparable between both groups (all P values greater than .05) (Figure 1E and G).

These data suggest that hypoxia does not affect growth or canonical marker expression in iPSC-PC.

The transcriptomic profile of iPSC-PC shows only minimal responses to hypoxia

To investigate the transcriptomic signature of iPSC-PC under hypoxia, we performed RNA-seq after 1 week of hypoxia. Overall, only 4.4% of all detected genes were differentially expressed genes (DEGs), with 1.7% upregulated and 2.7% downregulated in response to hypoxia (Figure 2A and B). As expected, genes and pathways associated with hypoxia were upregulated, including gene ontology terms "response to decreased oxygen levels," "response to oxygen levels," and "response to hypoxia" in iPSC-PC_{HYP} compared to iPSC-PC_{NORM} (Figure 2C).

Next, we explored whether genes encoding for canonical pericyte markers including PDGFR β (PDGFRB), Caldesmon (CALD1), NG2 (CSPG4), CD13 (ANPEP), and Vitronectin

(VTN) changed in response to hypoxia. Consistent with the histology data (Figure 1), we did not detect significant gene expression changes in canonical pericyte markers between iPSC-PC_{HYP} and iPSC-PC_{NORM} (all false discovery rates (FDR) values greater than 0.05, Figure 2D). We then examined whether hypoxia influenced the expression of genes encoding for major functional components of iPSC-PC including cell adhesion and tight junction proteins (Figure 2E and F). We found no significant changes in the expression of genes encoding for major junction proteins (DLG1, JAM3, JCAD, JUP, TJP2, all FDR values greater than >0.05) and adhesion junction proteins (ADGRA2, BCAM, CADM4, MCAM, SMAGP, all P values greater than .05) (Figure 2E and F). Among the genes most significantly upregulated upon hypoxia, we detected ICAM5 ($\log_2 FC=1.92$, FDR<0.001), HIF3A ($\log_2 FC=5.60$, FDR<0.001), CA9 ($\log_2 FC=4.35$, FDR=0.001), and TEK ($\log_2 FC=2.08$, FDR<0.001), which are known regulators of vascular adaptation to hypoxia (Figure 2G). Conversely, genes downregulated in response to hypoxia included GYS2 ($\log_2 FC=-6.69$, FDR<0.001), CHAC1 ($\log_2 FC=-5.87$, FDR<0.001), LAMP3 ($\log_2 FC=-5.87$, FDR<0.001), and CD36 ($\log_2 FC=-6.90$, FDR=3.08e-02), which are associated with reduced glucose and lipid metabolic processes (Figure 2G).

Given that hypoxia is known to influence various cellular processes beyond oxygen response, we conducted a gene set enrichment analysis (GSEA) to identify additional pathways affected by hypoxia. Primary pathways that were upregulated in response to hypoxia, aside from those related to hypoxia, included endocrine and hormonal regulation, immune responses, and vascular regulators (Figure 2H). In contrast, downregulated pathways were associated with biosynthetic processes including amino acid and lipid metabolism (Figure 2H), which is consistent with the observed DEGs.

Collectively, these data suggest that while hypoxia triggers expected oxygen-related responses and pathways associated with metabolism, it does not significantly impact the gene expression of canonical pericyte markers or key structural and functional components.

iPSC-PC functionally home to the mouse brain vasculature under hypoxia

The ability of iPSC-PC to wrap around brain capillaries is a prerequisite for pericyte-based therapies to restore the BBB integrity. To evaluate whether iPSC-PC retain their ability to functionally home to the mouse brain capillaries and form hybrid microvessels under hypoxic conditions, we used acute living brain slices from pericyte-deficient *Pdgfrb*F7/F7 mice and incubated them for 24 h with iPSC-PC under 3 conditions: (1) iPSC-PC_{NORM} with normoxic brain slices (iPSC-PC_{NORM} + BRAIN_{NORM}), (2) iPSC-PC_{HYP} with normoxic brain slices (iPSC-PC_{HYP} + BRAIN_{NORM}), and (3) iPSC-PC_{HYP} with hypoxic brain slices (iPSC-PC_{HYP} + BRAIN_{HYP}) to mimic the hypoxic host environment (Figure 3A and B).

We first quantified the percentage of iPSC-PC that homed to the host brain endothelium, distinguishing between those cells that formed processes along the vessels and those without processes. Across all groups, we found that a similar proportion of iPSC-PC homed with processes (iPSC-PC_{NORM} + BRAIN_{NORM}: 60.9 \pm 4.7%, iPSC-PC_{HYP} + BRAIN_{NORM}: 44.9 \pm 6.3%, iPSC-PC_{HYP} + BRAIN_{HYP}: 54.9 \pm 3.1%, P >.05) and homed without forming processes (iPSC-PC_{NORM} + BRAIN_{NORM}: 24.3 \pm 3.1%, iPSC-PC_{HYP} +

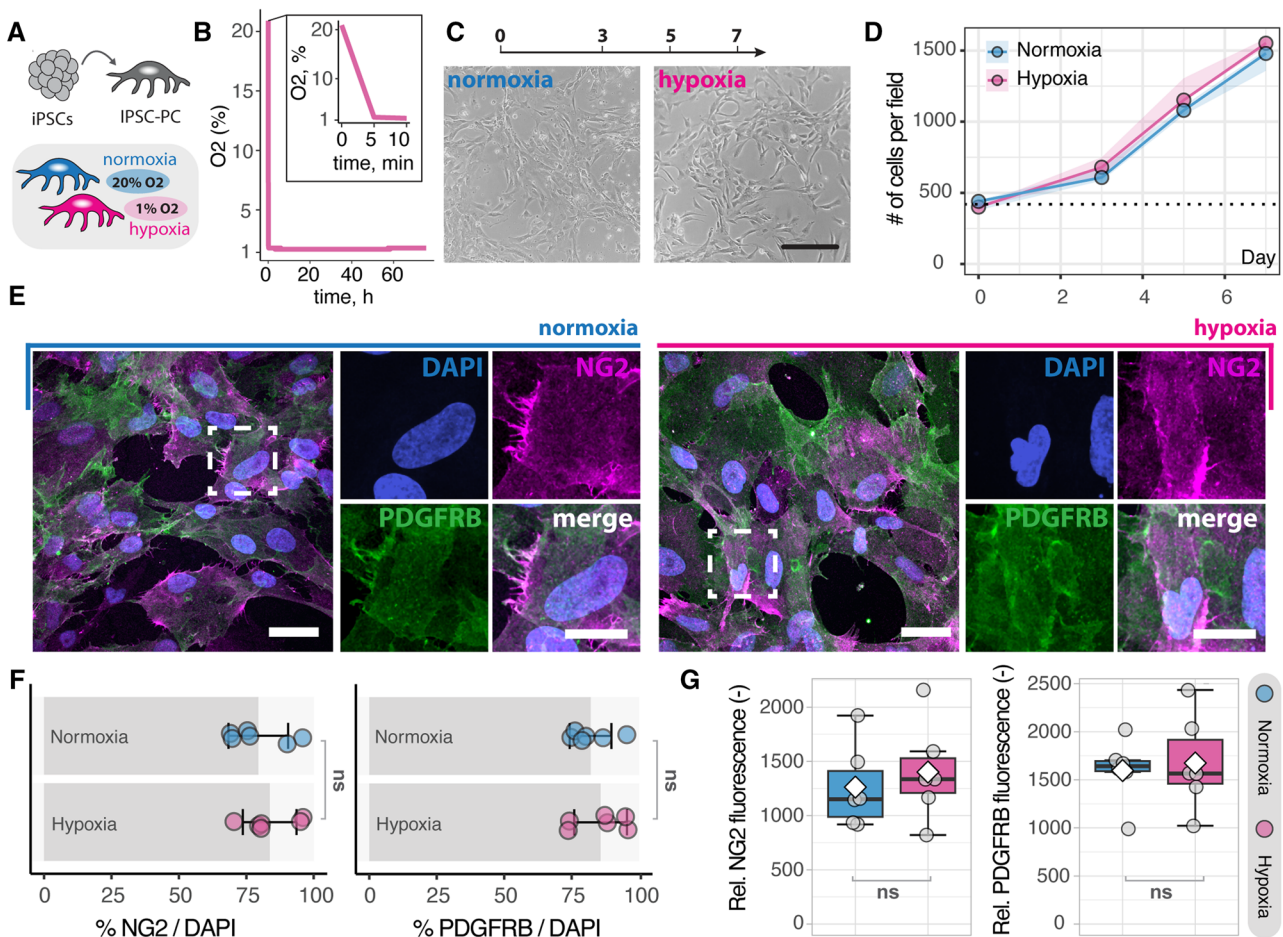


Figure 1. Growth and canonical marker expression of iPSC-PCs under hypoxia. (A) Schematic overview of the experimental setup. (B) Oxygen concentration in the hypoxia chamber over 72 h. (C) Representative images of iPSC-PCs at 7 days after hypoxia induction and normoxic iPSC-PC control. (D) Proliferation of iPSC-PCs at 0, 3, 5, and 7 days after hypoxia induction. Scale bar: 50 μm, n=3. (E) Fluorescence images of iPSC-PCs stained for the canonical pericyte markers NG2 (magenta) and PDGFRB (green), counterstained with DAPI (blue). Scale bar: 10 μm. (F) Quantification of the percentage of cells expressing NG2 and PDGFRB, n=6. (G) Relative fluorescence intensity of NG2 and PDGFRB under normoxia and hypoxia, n=6. Each dot represents an independent iPSC-PC culture. In line plots (D), the ribbon around each line plot represents the SEM. In box plots (F, G), the box represents the interquartile range, the horizontal line indicates the median, the white diamond represents mean, and whiskers show the minimum and maximum values. Statistical analysis was performed using a repeated measures mixed model for (D) and an unpaired t-test for (F, G). P>.05. Abbreviations: iPSC-PCs = pericytes derived from induced pluripotent stem cells; ns=nonsignificant.

BRAIN_{NORM}: 26.8±3.4%, iPSC-PC_{HYP} + BRAIN_{HYP}: 21.5±2.6%, P>.05). Only a minor fraction of iPSC-PC failed to home in all experimental groups (iPSC-PC_{NORM} + BRAIN_{NORM}: 14.8±1.8%, iPSC-PC_{HYP} + BRAIN_{NORM}: 28.3±3.5%, iPSC-PC_{HYP} + BRAIN_{HYP}: 23.5±4.7%, P>.05) (Figure 3C).

Next, we aimed to investigate whether the iPSC-PC can form functional interactions with the host endothelium of Pdgfrb^{F7/F7} mice. We performed PLA targeting known pericyte–endothelial cell interaction molecules, PDGFRB, and PDGF-BB^{34–36} (Figure 3D). Proximity ligation assay signal of PDGFRB/PDGFB was detectable in all 3 experimental groups at the pericyte–endothelial interface (PDGFRB⁺ Lectin⁺), suggesting the formation of functional pericyte–endothelial contacts in all 3 experimental conditions (Figure 3E).

IPSC-PC phagocytic properties of Aβ neurotoxins remain unchanged under hypoxia

Previous studies suggest that pericytes can phagocytose Aβ in vitro.^{15,37,38} Therefore, we aimed to test whether iPSC-PC have

comparable Aβ clearance properties under normoxic and hypoxic conditions. We used consecutive frozen brain sections from 10-month-old 5×FAD mice, which are known to have significant Aβ pathology at this age,^{39,40} and incubated these sections with iPSC-PC_{NORM} and iPSC-PC_{HYP} to these sections for 24 h. Brain sections from 5×FAD mice without cells served as a negative control (Figure 4A). After confirming the presence of iPSC-PC on the brain sections after 24 h, we quantified the Aβ load in the cortex and hippocampus (Figure 4B). We observed a similar reduction in Aβ levels, which decreased from 32.2±1.5% in the control group to 21.7±0.5% in iPSC-PC_{NORM} (P<.01) and to 23.9±1.7% in iPSC-PC_{HYP}, (P<.05) in the cortex (Figure 4C). A similar trend was observed in the hippocampus, with Aβ levels reduced from 24.3±1.3% in the control to 20.1±0.7% (iPSC-PC_{HYP}, P=.2, Figure 4C) after cell incubations. Notably, no significant differences in Aβ uptake were observed between iPSC-PC under normoxic and hypoxic conditions, suggesting similar phagocytic properties in both environments (all P values greater than .05, Figure 4C).

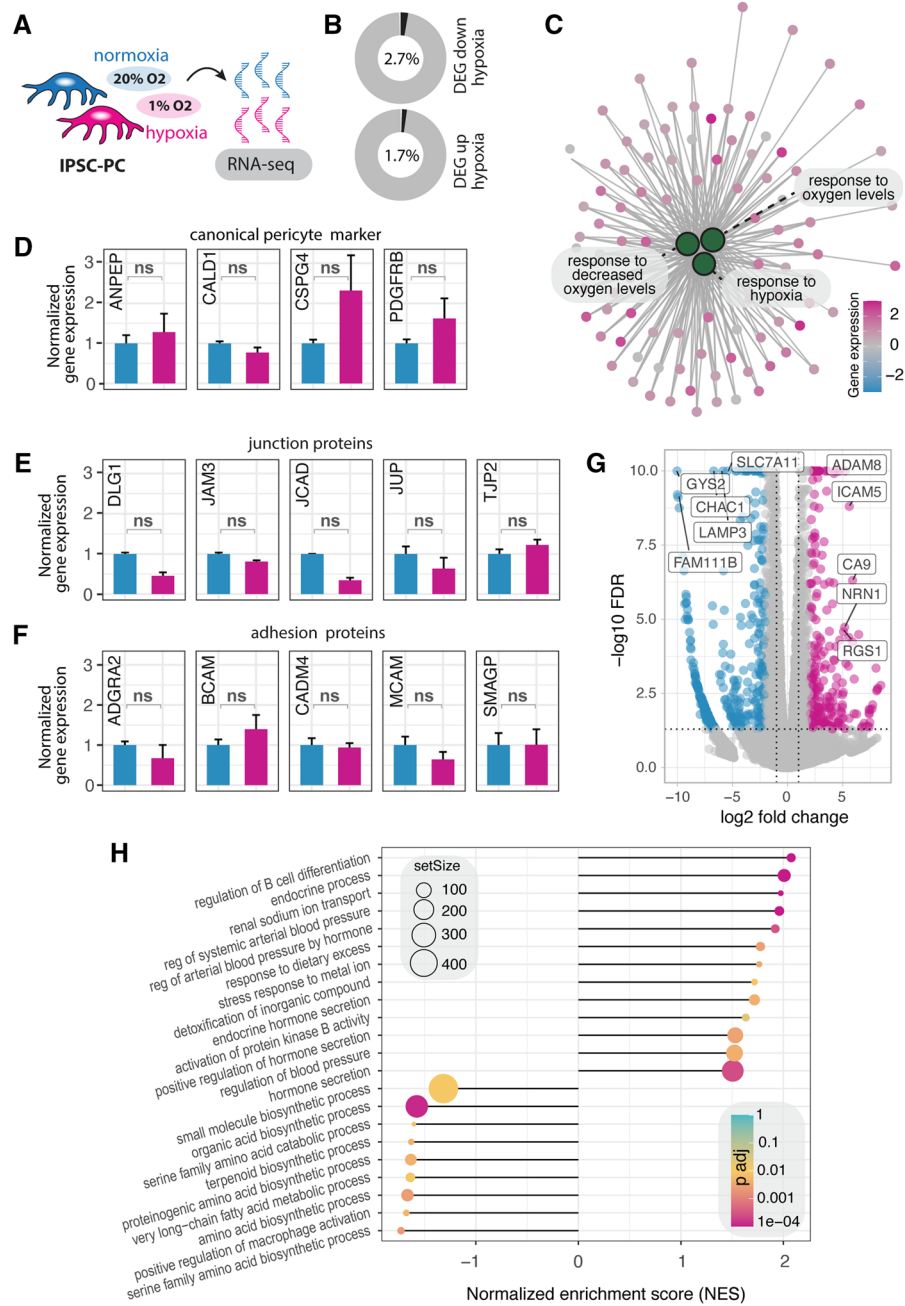


Figure 2. Transcriptomic analysis of iPSC-PCs under hypoxia. (A) Experimental setup for RNA sequencing after 1 week of hypoxia. (B) Percentage of differentially expressed genes (DEGs) in iPSC-PC_{HYP} compared to iPSC-PC_{NORM}. (C) Gene interaction network highlighting hypoxia-responsive genes (small dots) within enriched pathways related to hypoxia (large green dots) upregulated in iPSC-PC_{HYP}. (D) Normalized expression levels of canonical pericyte markers in iPSC-PC_{HYP} and iPSC-PC_{NORM}. (E) Expression levels of key junction proteins in iPSC-PC_{HYP} and iPSC-PC_{NORM}. (F) Expression levels of adhesion in iPSC-PC_{HYP} and iPSC-PC_{NORM}. (G) Volcano plot showing DEGs, with selected DEG labeled (magenta, upregulated; blue, downregulated). (H) Gene set enrichment analysis (GSEA) showing most upregulated and downregulated in iPSC-PC_{HYP} and iPSC-PC_{NORM}. Data represent $n=6$ independent cultures. Genes with $\text{FDR} < 0.05$ and $|\log_2 \text{FC}| > 1.5$ were considered significantly differentially expressed. Abbreviations: iPSC-PCs = pericytes derived from induced pluripotent stem cells; ns = nonsignificant.

Discussion

In this study, we show that iPSC-PC retain their major molecular and functional properties under 1 week of severe hypoxia. We identified similar growth rates, expression of canonical pericyte markers and junctional and adhesion proteins were unaffected by hypoxia. Additionally, iPSC-PC can home to pericyte-deficient host vessels in a hypoxic environment and have similar phagocytic properties of A β to normoxic iPSC-PC.

Traditionally, brain pericytes have been considered to be highly susceptible to hypoxia as they are often the first non-neuronal cell types lost after severe hypoxia, for example, after experimental stroke^{26,27,41,42} or pathological CBF changes in dementias^{24,43,44} contributing to BBB disruption and subsequent neurodegeneration.¹ Therefore, transplantation of pericytes is an interesting therapeutic target to restore the BBB; however, it was uncertain whether iPSC-PC can retain their functional

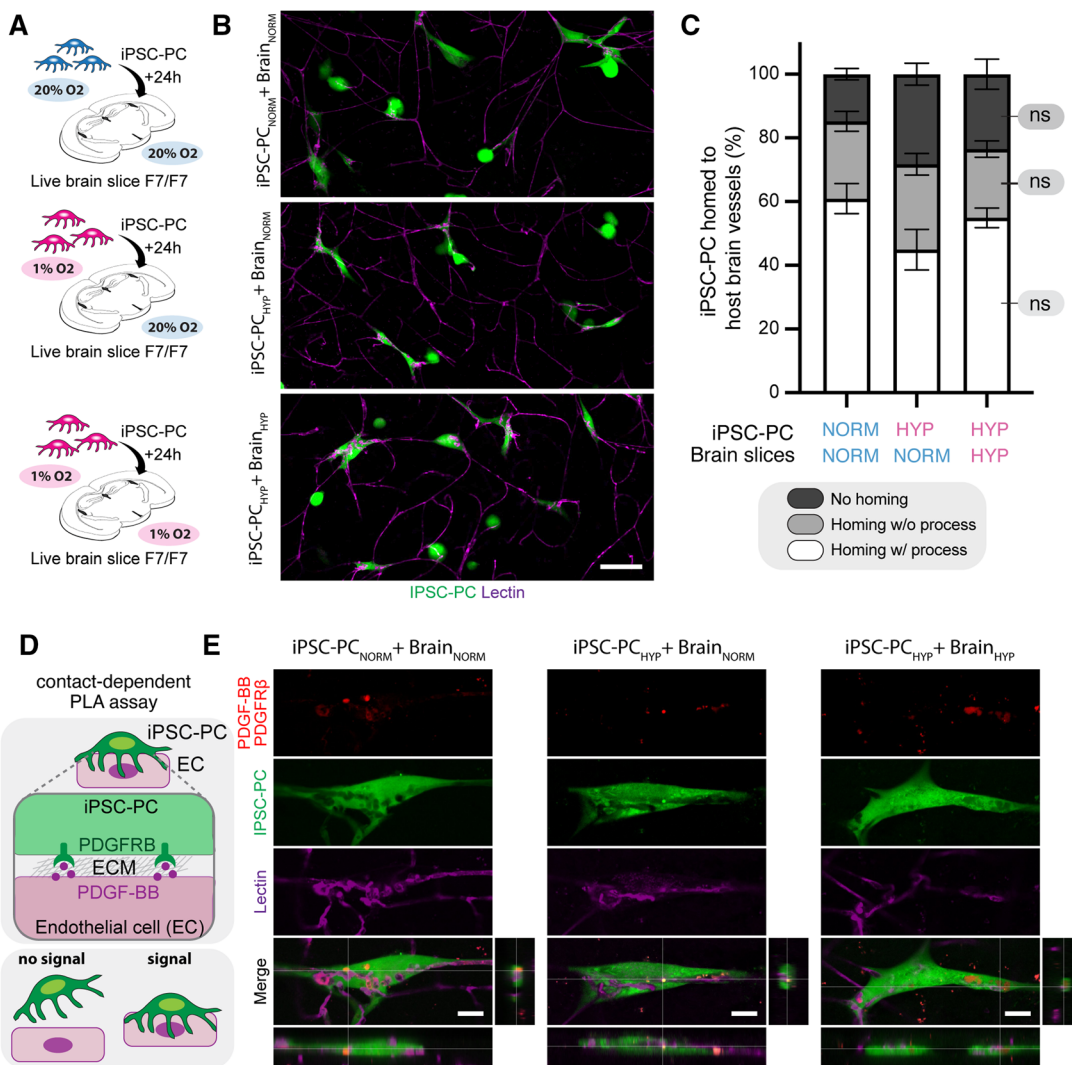


Figure 3. iPSC-PC home to brain capillaries and form functional hybrid microvessels under normoxia and hypoxia. (A) Schematic overview of experimental setup. Acute brain slices from pericyte-deficient *Pdgfrb*F7/F7 mice were incubated with iPSC-PC under 3 conditions: (1) iPSC-PC_{NORM} + BRAIN_{NORM}, (2) iPSC-PC_{HYP} + BRAIN_{NORM}, and (3) iPSC-PC_{HYP} + BRAIN_{HYP}. (B) Representative confocal images showing iPSC-PC (green, CellTracker) interacting with host brain capillaries (magenta, Lectin). Scale bar: 20 μm. (C) Quantification of iPSC-PC homing and process formation with the host brain endothelium across conditions. (D) Schematic of the proximity ligation assay (PLA) used to assess pericyte–endothelial cell contact of PDGFRB (pericytes) and PDGF-BB (endothelium). (E) Representative PLA images showing PDGFRB-PDGF-BB colocalization (red) at the pericyte–endothelial interface under all 3 conditions, confirming functional interaction. Scale bar: 5 μm. Data represent $n=4$ independent cell cultures for each condition. Statistical significance was determined by 1-way ANOVA followed by Tukey's post hoc test. Abbreviations: iPSC-PCs = pericytes derived from induced pluripotent stem cells; ns = nonsignificant.

properties in the hypoxic microenvironment. While a recent study showed that transplantation of mouse pericytes can increase CBF and reduce Aβ pathology in amyloid model mice,⁴⁵ the study used mesoderm-derived pericytes. However, in major neurological disorders including stroke and AD, pericyte degeneration is often observed in the cortex and hippocampus, which primarily affects forebrain NCC-derived pericytes, but not mesodermal pericytes.⁴⁶ Our data now show that NCC-derived iPSC-PC, which have been previously shown to closely resemble NCC-derived primary forebrain pericytes,¹⁵ can also sustain an hypoxic environment.

We observed in hypoxic iPSC-PC energy metabolic reprogramming, which has been previously observed in vascular cells, favoring, for example, glycolysis over oxidative phosphorylation.^{47,48} Additionally, upregulation of *ICAM5*, *HIF3A*, *CA9*, and *TEK* in hypoxia-exposed pericytes could suggest an

adaptive mechanism to maintain vascular support.^{49,50} Furthermore, hypoxic iPSC-PC maintained expression of the important pericyte–endothelial communication signaling of PDGFRB and PDGF-BB, which has been previously described to be important for maintaining the BBB-supporting functions of pericytes.^{34–36} While we identified the molecular signature of hypoxic iPSC-PC and their interaction with endothelial cells, we used a simplified *in vitro* model with reduced (1% O₂) concentration and *ex vivo* brain slices; however, *in vivo* validation should be performed in future studies to assess iPSC-PC physiological integration to the host vasculature and therapeutic efficacy. Additionally, while our study examined the response of iPSC-PC for 1 week after hypoxia, prolonged hypoxia may induce additional changes in iPSC-PC that need further exploration. Although we quantified the proportion of iPSC-PCs that home to host vasculature, we did not perform spatial mapping to determine

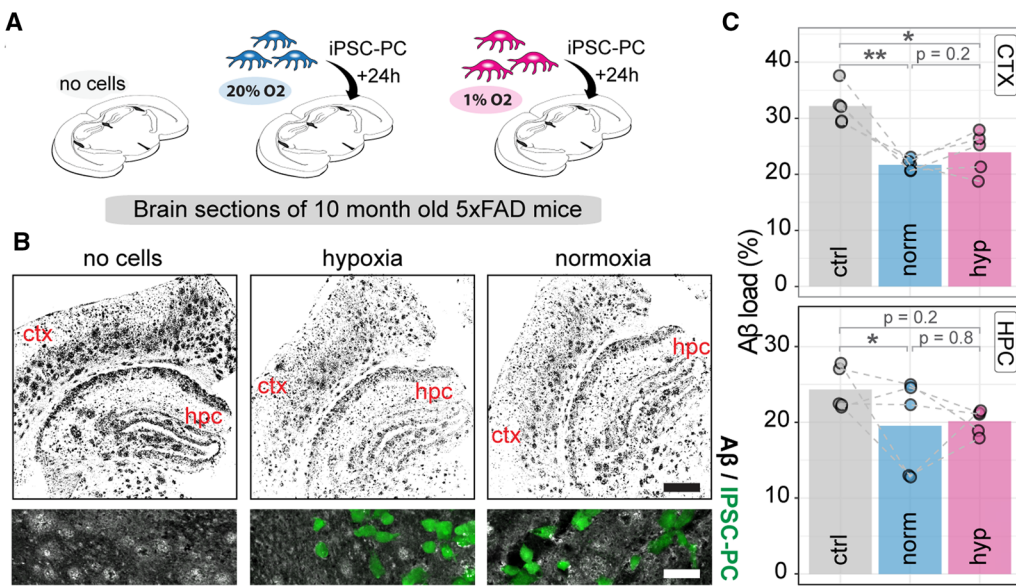


Figure 4. IPSC-PC phagocytose A β from brain sections of aged 5xFAD mice under normoxia and hypoxia. (A) Schematic overview of experimental setup. Frozen brain sections from 10-month-old 5xFAD mice were incubated with iPSC-PC under 3 conditions: (1) no cells, (2) iPSC-PC_{NORM} and (3) iPSC-PC_{HYP}. (B) Representative confocal images showing A β (black). Magnification view within the section showing iPSC-PC (green, CellTracker) and A β (gray). Scale bar: overview: 200 μ m, zoom in: 50 μ m (C) Quantification of A β load (%) in the cortex (ctx) and hippocampus (hpc). Each dot represents an individual brain section, with dotted lines connecting paired consecutive sections from the same brain region across conditions. Data represent n=5 independent cell cultures for each condition. Bars represent mean, each dot represents iPSC-PC added to a different brain slice. Dashed lines indicate consecutive brain sections. Asterisks indicate significance: *P<.05, **P<.01 using paired t-test with correction for multiple testing. Abbreviations: A β = amyloid beta; iPSC-PCs = pericytes derived from induced pluripotent stem cells.

whether iPSC-PCs preferentially localize to branch points or associate with residual endogenous pericytes in Pdgfrb^{F/F} mice. Future studies may address these important interactions. Future studies could also explore the addition of normoxic iPSC-PCs to hypoxic brain tissue, as this would be important to understand how cultured iPSC-PCs function in a hypoxic environment and whether their molecular and functional properties are maintained after transplantation.

Previous work has shown that pericytes can phagocytose A β in vitro,^{15,37,38} which is in accordance with our findings. We additionally show that iPSC-PC retain their A β phagocytic properties under hypoxia indicating that iPSC-PC could take up A β even in the presence of a low-oxygen environment in AD. Future studies could confirm these findings in AD mouse models to assess iPSC-PC therapeutic potential in vivo. Potentially, the ability of iPSC-PC to improve the vascular and A β pathology in AD could also be tested in new AD mouse models with a stronger vascular phenotype.⁵¹ In our A β phagocytosis assay, while we observed a reduction in A β after iPSC-PC exposure, we did not quantify the spatial relationship between iPSC-PCs and A β plaques or vessels. Future work will be necessary to determine whether A β clearance is driven primarily by perivascular interactions or plaque-associated phagocytosis.

In conclusion, the present study provides support that iPSC-PC maintain their major functional properties under hypoxia. Therefore, iPSC-PC might be a suitable cell source for future brain transplants for neurological disorders that are associated with pericyte deficiency and hypoxia such as stroke, AD, and other related disorders.

Author contributions

Mingzi Zhang (Conceptualization, Data curation, Formal analysis, Investigation, Methodology), Youbin Kim (Conceptualization, Data curation, Formal analysis, Investigation,

Methodology), Allison Bosworth (Data curation, Formal analysis), Julia Tcw (Methodology), Lina R. Nih (Methodology), Kassandra Kisler (Investigation, Methodology), Abhay P. Sagare (Investigation, Methodology), and Ruslan Rust (Conceptualization, Data curation, Formal analysis, Funding acquisition, Investigation, Methodology, Project administration)

Funding

R.R. acknowledges funding support from Swiss 3R Competence Center (OC-2020-002), the Swiss National Science Foundation (CRSK-3_195902, PZ00P3_216225) and Keck School of Medicine (KSOM) Dean's Pilot Funding Program Award. J.T. acknowledges funding support from NIH NIA R01AG082362, R01AG083941, U19AG069701.

Conflicts of interest

None declared.

Data availability

All data are available upon request. RNA-seq data will be made publicly available on NCBI GEO.

References

1. Armulik A, Genové G, Mäe M, et al. Pericytes regulate the blood-brain barrier. *Nature*. 2010;468:557-561.
2. Daneman R, Zhou L, Kebede AA, Barres BA. Pericytes are required for blood-brain barrier integrity during embryogenesis. *Nature*. 2010;468:562-566.
3. Bell RD, Winkler EA, Sagare AP, et al. Pericytes control key neurovascular functions and neuronal phenotype in the adult brain and during brain aging. *Neuron*. 2010;68:409-427.

4. Hall CN, Reynell C, Gesslein B, et al. Capillary pericytes regulate cerebral blood flow in health and disease. *Nature*. 2014;508:55-60.
5. Ayloo S, Lazo CG, Sun S, et al. Pericyte-to-endothelial cell signaling via vitronectin-integrin regulates blood-CNS barrier. *Neuron*. 2022;110:1641-1655.e6.
6. Rust R, Yin H, Achón Buil B, Sagare A, Kisler K. The blood-brain barrier: a help and a hindrance. *Brain*. 2025;148:2262-2282. <https://doi.org/10.1093/brain/awaf068>
7. Rust R, Sagare AP, Zhang M, Zlokovic BV, Kisler K. The blood-brain barrier as a treatment target for neurodegenerative disorders. *Exp Opin Drug Deliv*. 2025;22:673-692.
8. Lacoste B, Prat A, Freitas-Andrade M, Gu C. The blood-brain barrier: composition, properties, and roles in brain health. *Cold Spring Harb Perspect Biol*. 2025;17. <https://doi.org/10.1101/cshperspect.a041422>
9. Nadareishvili Z, Simpkins AN, Hitomi E, Reyes D, Leigh R. Post-stroke blood-brain barrier disruption and poor functional outcome in patients receiving thrombolytic therapy. *Cerebrovasc Dis*. 2019;37:135-142.
10. Nation DA, Sweeney MD, Montagne A, et al. Blood-brain barrier breakdown is an early biomarker of human cognitive dysfunction. *Nat Med*. 2019;25:270-276.
11. Montagne A, Nation DA, Sagare AP, et al. APOE4 leads to blood-brain barrier dysfunction predicting cognitive decline. *Nature*. 2020;581:71-76.
12. Kirabali T, Rust R, Rigotti S, et al. Distinct changes in all major components of the neurovascular unit across different neuropathological stages of Alzheimer's disease. *Brain Pathol*. 2020;30:1056-1070. <https://doi.org/10.1111/bpa.12895>
13. Faal T, Phan DTT, Davtyan H, et al. Induction of mesoderm and neural crest-derived pericytes from human pluripotent stem cells to study blood-brain barrier interactions. *Stem Cell Rep*. 2019;12:451-460.
14. Stebbins MJ, Gastfriend BD, Canfield SG, et al. Human pluripotent stem cell-derived brain pericyte-like cells induce blood-brain barrier properties. *Sci Adv*. 2019;5:eau7375.
15. Rust R, Sagare AP, Kisler K, et al. Molecular signature and functional properties of human pluripotent stem cell-derived brain pericytes. *bioRxiv* 546577. <https://doi.org/10.1101/2023.06.26.546577>, 2025, preprint: not peer reviewed.
16. Sun J, Huang Y, Gong J, et al. Transplantation of iPSC-derived pericyte-like cells promotes functional recovery in ischemic stroke mice. *Nat Commun*. 2020;11:5196.
17. Kirabali T, Rust R. iPSC-derived pericytes for neurovascular regeneration. *Eur J Clin Invest*. 2021;51:e13601.
18. Markus R, Reutens DC, Kazui S, et al. Hypoxic tissue in ischaemic stroke: persistence and clinical consequences of spontaneous survival. *Brain*. 2004;127:1427-1436.
19. Bracko O, Cruz Hernández JC, Park L, Nishimura N, Schaffer CB. Causes and consequences of baseline cerebral blood flow reductions in Alzheimer's disease. *J Cereb Blood Flow Metab*. 2021;41:1501-1516.
20. Tallquist MD, French WJ, Soriano P. Additive effects of PDGF receptor beta signaling pathways in vascular smooth muscle cell development. *PLoS Biol*. 2003;1:E52.
21. Winkler EA, Bell RD, Zlokovic BV. Pericyte-specific expression of PDGF beta receptor in mouse models with normal and deficient PDGF beta receptor signaling. *Mol Neurodegener*. 2010;5:32.
22. du Sert NP, Hurst V, Ahluwalia A, et al. The ARRIVE guidelines 2.0: updated guidelines for reporting animal research. *J Cereb Blood Flow Metab*. 2020;40:1769-1777.
23. Tcw J, Qian L, Pipalia NH, et al. Cholesterol and matrisome pathways dysregulated in astrocytes and microglia. *Cell*. 2022;185:2213-2233.e25.
24. Nikolakopoulou AM, Zhao Z, Montagne A, Zlokovic BV. Regional early and progressive loss of brain pericytes but not vascular smooth muscle cells in adult mice with disrupted platelet-derived growth factor receptor-β signaling. *PLoS One*. 2017;12:e0176225.
25. Otsu N. A threshold selection method from gray-level histograms. *IEEE Trans Syst Man Cybern*. 1979;9:62-66.
26. Rust R, Grönnert L, Gantner C, et al. Nogo—a targeted therapy promotes vascular repair and functional recovery following stroke. *Proc Natl Acad Sci U S A*. 2019;116:14270-14279. <https://doi.org/10.1073/pnas.1905309116>
27. Weber RZ, Buil BA, Rentsch NH, et al. Human iPSC-derived cell grafts promote functional recovery by molecular interaction with stroke-injured brain. *bioRxiv* 588020. <https://doi.org/10.1101/2024.04.03.588020>, 2024, preprint: not peer reviewed.
28. Weber RZ, Achón Buil B, Rentsch NH, et al. A molecular brain atlas reveals cellular shifts during the repair phase of stroke. *bioRxiv* 608971. <https://doi.org/10.1101/2024.08.21.608971>, 2025, preprint: not peer reviewed.
29. Rust R, Weber RZ, Generali M, et al. Xeno-free induced pluripotent stem cell-derived neural progenitor cells for in vivo applications. *J Transl Med*. 2022;20:421.
30. Weber RZ, Mulders G, Perron P, Tackenberg C, Rust R. Molecular and anatomical roadmap of stroke pathology in immunodeficient mice. *bioRxiv* 501836. <https://doi.org/10.1101/2022.07.28.501836>, 2022, preprint: not peer reviewed.
31. Rust R. Ischemic stroke-related gene expression profiles across species: a meta-analysis. *J Inflamm (Lond)*. 2023;20:21.
32. Robinson MD, McCarthy DJ, Smyth GK. edgeR: a bioconductor package for differential expression analysis of digital gene expression data. *Bioinformatics*. 2010;26:139-140.
33. Wu T, Hu E, Xu S, et al. clusterProfiler 4.0: a universal enrichment tool for interpreting omics data. *Innovation (Camb)*. 2021;2:100141.
34. Smyth LCD, Hight B, Jansson D, et al. Characterisation of PDGF-BB: PDGFRβ signalling pathways in human brain pericytes: evidence of disruption in Alzheimer's disease. *Commun Biol*. 2022;5:235.
35. Shen J, Xu G, Zhu R, et al. PDGFR-β restores blood-brain barrier functions in a mouse model of focal cerebral ischemia. *J Cereb Blood Flow Metab*. 2019;39:1501-1515.
36. Jansson D, Scotter EL, Rustenhoven J, et al. Interferon-γ blocks signalling through PDGFRβ in human brain pericytes. *J Neuroinflammation*. 2016;13:249.
37. Ma Q, Zhao Z, Sagare AP, et al. Blood-brain barrier-associated pericytes internalize and clear aggregated amyloid-β42 by LRP1-dependent apolipoprotein E isoform-specific mechanism. *Mol Neurodegener*. 2018;13:57.
38. Ding Y, Palecek SP, Shusta EV. iPSC-derived blood-brain barrier modeling reveals APOE isoform-dependent interactions with amyloid beta. *Fluids Barriers CNS*. 2024;21:79.
39. Oakley H, Cole SL, Logan S, et al. Intraneuronal β-amyloid aggregates, neurodegeneration, and neuron loss in transgenic mice with five familial Alzheimer's disease mutations: potential factors in amyloid plaque formation. *J Neurosci*. 2006;26:10129-10140.
40. Forner S, Kawauchi S, Balderrama-Gutierrez G, et al. Systematic phenotyping and characterization of the 5xFAD mouse model of Alzheimer's disease. *Sci Data*. 2021;8:270.
41. Weber RZ, Grönnert L, Mulders G, et al. Characterization of the blood brain barrier disruption in the photothrombotic stroke model. *Front Physiol*. 2020;11:586226.
42. Nih LR, Gojgini S, Carmichael ST, Segura T. Dual-function injectable angiogenic biomaterial for the repair of brain tissue following stroke. *Nat Mater*. 2018;17:642-651.
43. Shi H, Koronyo Y, Rentsendorj A, et al. Identification of early pericyte loss and vascular amyloidosis in Alzheimer's disease retina. *Acta Neuropathol*. 2020;139:813-836.
44. Ding R, Hase Y, Ameen-Ali KE, et al. Loss of capillary pericytes and the blood-brain barrier in white matter in poststroke and vascular dementias and Alzheimer's disease. *Brain Pathol*. 2020;30:1087-1101.
45. Tachibana M, Yamazaki Y, Liu C-C, Bu G, Kanekiyo T. Pericyte implantation in the brain enhances cerebral blood flow and reduces amyloid-β pathology in amyloid model mice. *Exp Neurol*. 2018;300:13-21.

46. Girolamo F, de Trizio I, Errede M, *et al.* Neural crest cell-derived pericytes act as pro-angiogenic cells in human neocortex development and gliomas. *Fluids Barriers CNS*. 2021;18:14.
47. Shi Z, Hu C, Zheng X, Sun C, Li Q. Feedback loop between hypoxia and energy metabolic reprogramming aggravates the radio-resistance of cancer cells. *Exp Hematol Oncol*. 2024;13:55.
48. Wu D, Huang R-T, Hamanaka RB, *et al.* HIF-1 α is required for disturbed flow-induced metabolic reprogramming in human and porcine vascular endothelium. *Elife*. 2017;6:e25217.
49. Li Y, Girard R, Srinath A, *et al.* Transcriptomic signatures of individual cell types in cerebral cavernous malformation. *Cell Commun Signal*. 2024;22:23.
50. Heng JS, Rattner A, Stein-O'Brien GL, *et al.* Hypoxia tolerance in the Norrin-deficient retina and the chronically hypoxic brain studied at single-cell resolution. *Proc Natl Acad Sci U S A*. 2019;116:9103-9114.
51. Szu JI, Obenaus A. Cerebrovascular phenotypes in mouse models of Alzheimer's disease. *J Cereb Blood Flow Metab*. 2021;41: 1821-1841.